Available online at www.sciencedirect.com
SCIENCE DIRECT®
Engineering Structures 26 (2004) 1043–1054
ENGINEERING STRUCTURES
www.elsevier.com/locate/engstruct

Finite strip modeling for optimal design of prestressed folded plate structures

Alessio Bergamini [a], Fabio Biondini [b,*]

[a] Consultant Engineer, Via F. Turati, 23, 24057 Martinengo (BG), Italy
[b] Department of Structural Engineering, Technical University of Milan, Piazza L. da Vinci, 32, 20133 Milan, Italy

Received 29 July 2003; received in revised form 29 January 2004; accepted 5 March 2004

Abstract

The optimal limit state design of prestressed thin-walled folded plate structures under multiple loading conditions is presented. The design variables include (a) geometrical quantities, like the thickness and the dimensions of the structural members, (b) topological parameters, which define the location and the connectivity of such elements, and (c) the characteristics of the eventual prestressing system, described by the prestressing forces and the cables profile. Besides the physical and technological limits on such variables, the design constraints account for given limit states on both the stress and the displacement states which define the structural behavior. The objective of the design process is to find the structural layout which minimizes the structural volume and/or the total prestressing force according to the mentioned side and behavioral constraints. The solution of the corresponding non-linear optimization problem is achieved by using a numerical procedure based on the complex method. The structural analyses required during the optimization process are performed by using the finite strip method. Some applications to the optimal design of beams, vaults and box-girder bridges show the effectiveness of the proposed procedure.

Keywords: Folded plate structures; Finite strip method; Prestressing; Structural optimization; Complex method

1. Introduction

Design, construction and management of every engineering system usually involve several technological and managerial decisions aimed to minimize the required effort or maximize the desired benefit. In structural design, the importance of this optimization process is emphasized when the scheme of the carrying mechanism follows the shape of the structure itself, becoming in this way a direct expression of its functional requirements. Clearly, the complexity of the design choices involved in this phase depends on the typology of the considered structural system.

There is a great deal of structures for which both the geometry and the material properties can be considered constants along a main direction, straight or curved, while, generally, only the loading distribution may vary. In many cases, the performance of these structures is also improved by means of proper longitudinal prestressing systems. Fig. 1 shows some of these structural types, which refer to thin-walled beams, cylindrical and prismatic shell roofs [1] and box-girder bridges [6,9,13]. For these structures, the design process should lead to define the optimal morphology of the transversal cross-section, which means its geometry, size, shape and topology, as well as the layout of the prestressing system, described by the prestressing forces and the cables profile.

In such context, the attention of this paper is focussed on the optimal design of thin-walled prestressed structures composed by folded plates and subjected to multiple loading conditions [3,4]. A proper modeling of these structures can be found within the framework of the finite strip method (Fig. 2). As well known, this method is based on the formulation of a special class of finite elements as long as the structure and interconnected along the nodal lines that constitute the sides of the strips themselves [5,7,8]. As for many other

* Corresponding author. Tel.: +39-02-2399-4394; fax: +39-02-2399-4220.
E-mail address: biondini@stru.polimi.it (F. Biondini).

0141-0296/$ - see front matter © 2004 Elsevier Ltd. All rights reserved.
doi:10.1016/j.engstruct.2004.03.005

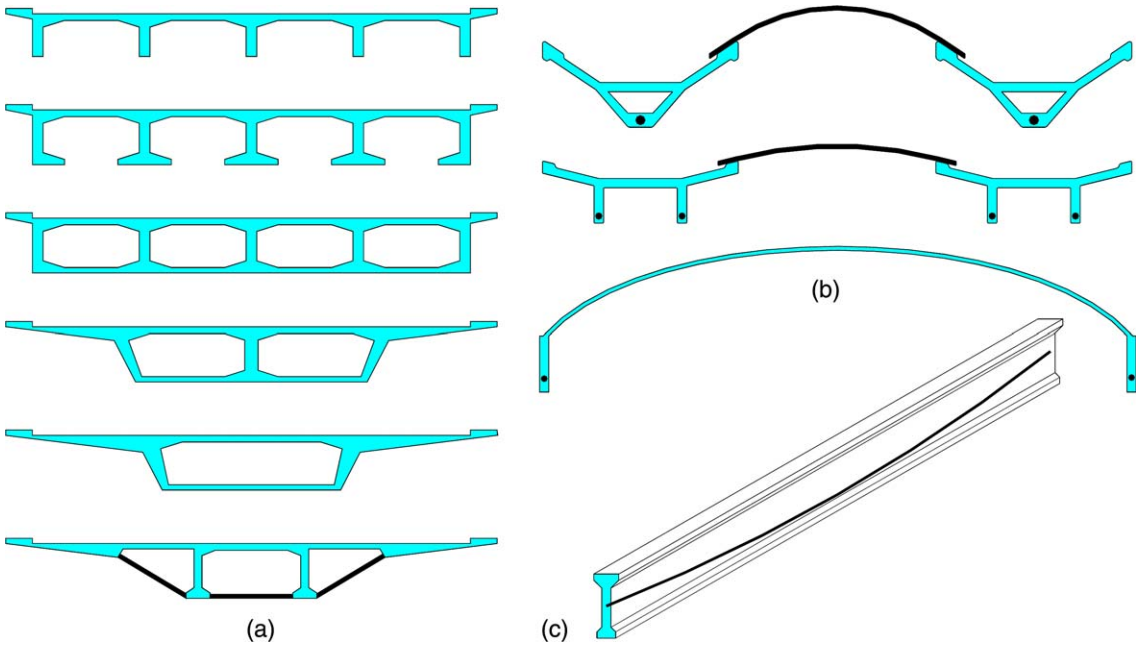

Fig. 1. Some examples of structures for which both the geometry and the material properties can be considered constants along a main direction. (a) Bridge decks with prestressed girders and box-girder bridges; (b) Prestressed prismatic and cylindrical shell roofs; (c) Prestressed thin-walled beams.

classical modeling techniques, eventual prestressing systems can also be properly modeled by means of a set of loads equivalent to the prestressing actions taking both instantaneous and time dependent losses into account. Based on such kind of modeling, the choice of the design variables considers (a) geometrical quantities, like the thickness and the dimensions of the finite strips, (b) topological parameters, which define the location and the connectivity of such elements, and (c) the characteristics of the eventual prestressing system, described by the prestressing forces and the cables profile. In particular, the design space of feasible structural morphologies is restricted to satisfy physical and technological limits on the design variables, as well as given limit states on both the stress and the displacement states which define the structural behavior at the serviceability stage. In the selection of these design constraints, special attention is paid to the definition of a proper deformability index which accounts for the particular nature of the structures investigated in the present work. The optimal choice within this set of feasible solutions is based on the definition of an objective function to be minimized which represents a weighted sum of the structural volume and the total prestressing force. The solution of the corresponding non-linear optimization problem is achieved by using a numerical procedure based on the well-known complex method [2,12].

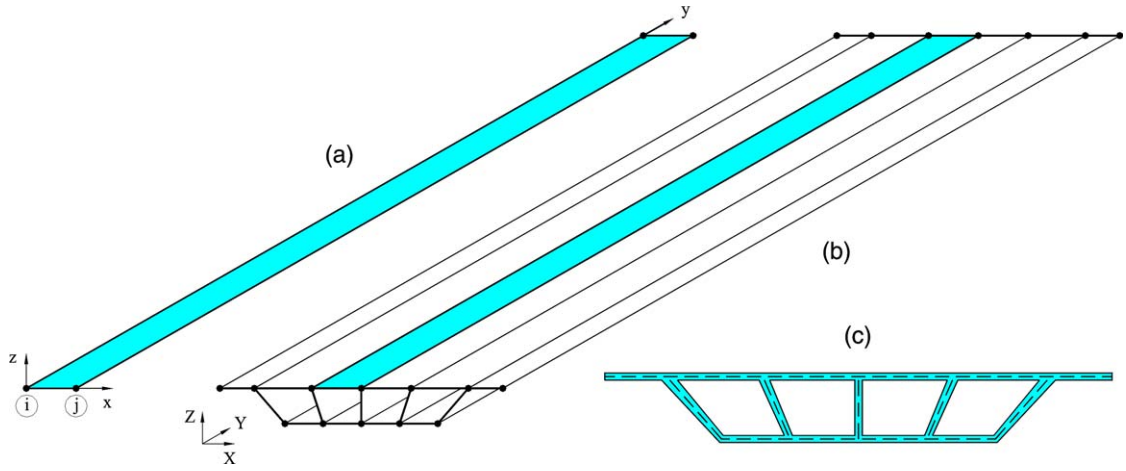

Fig. 2. Reference systems and finite element model. (a) Finite strip element between the nodal lines i and j in the local reference system (x,y,z); (b) Finite strip modeling of the structure in the global reference system (X,Y,Z); (c) Thickness distribution of the cross-section.

In the following, the general criteria of the structural modeling and the basic formulation of the proposed design methodology are presented and explained. Special attention is paid to the choice of the design variables, the definition of the design constraints and the formulation of the objective function. The effectiveness of the proposed methodology is finally proven by some applications to the optimal design of beams, vaults and box-girder bridges.

2. Formulation of the optimization problem

The problem of the optimum structural design consists of finding a set of design variables which accounts for assigned design constraints and optimizes one or more given target requirements. Therefore, from a mathematical point of view, the purpose of the design process is to find a vector $\boldsymbol{x}$ which optimizes the value of an objective function $f(\boldsymbol{x})$, according to either side constraints with bounds $\boldsymbol{x}^-$ and $\boldsymbol{x}^+$, or inequality $\boldsymbol{g}(\boldsymbol{x}) \leq \boldsymbol{0}$ and/or equality $\boldsymbol{h}(\boldsymbol{x}) = \boldsymbol{0}$ behavioral constraints. Since, without any loss of generality, minimization problems only may be considered, the previous optimization problem is cast in the following form:

$$\min_{\mathbf{x}}\{f(\boldsymbol{x})|\boldsymbol{x}^- \leq \boldsymbol{x} \leq \boldsymbol{x}^+, \boldsymbol{g}(\boldsymbol{x}) \leq \boldsymbol{0}, \boldsymbol{h}(\boldsymbol{x}) = \boldsymbol{0}\} \quad (1)$$

which, in the general case, represents a non-linear programming problem.

2.1. Choice of the design variables

In structural design, the choice of the design variables represents a crucial point which drives the whole design process. For the class of structures considered here, the design variables can be conveniently defined on the base of the finite strip model adopted for the structural analyses. This means that the design model and the analysis model are strongly related between them, even if they express different points of view of the structural problem. Specifically, the analysis model is defined as a set of folded plates interconnected to each other in the longitudinal direction along one of their external nodal lines. Therefore, the design variables which define the design model can be chosen as described in the following points (Fig. 3):

- The *structural shape* is directly defined by the location of the nodal lines.
- The *structural size* is related to the thickness of the

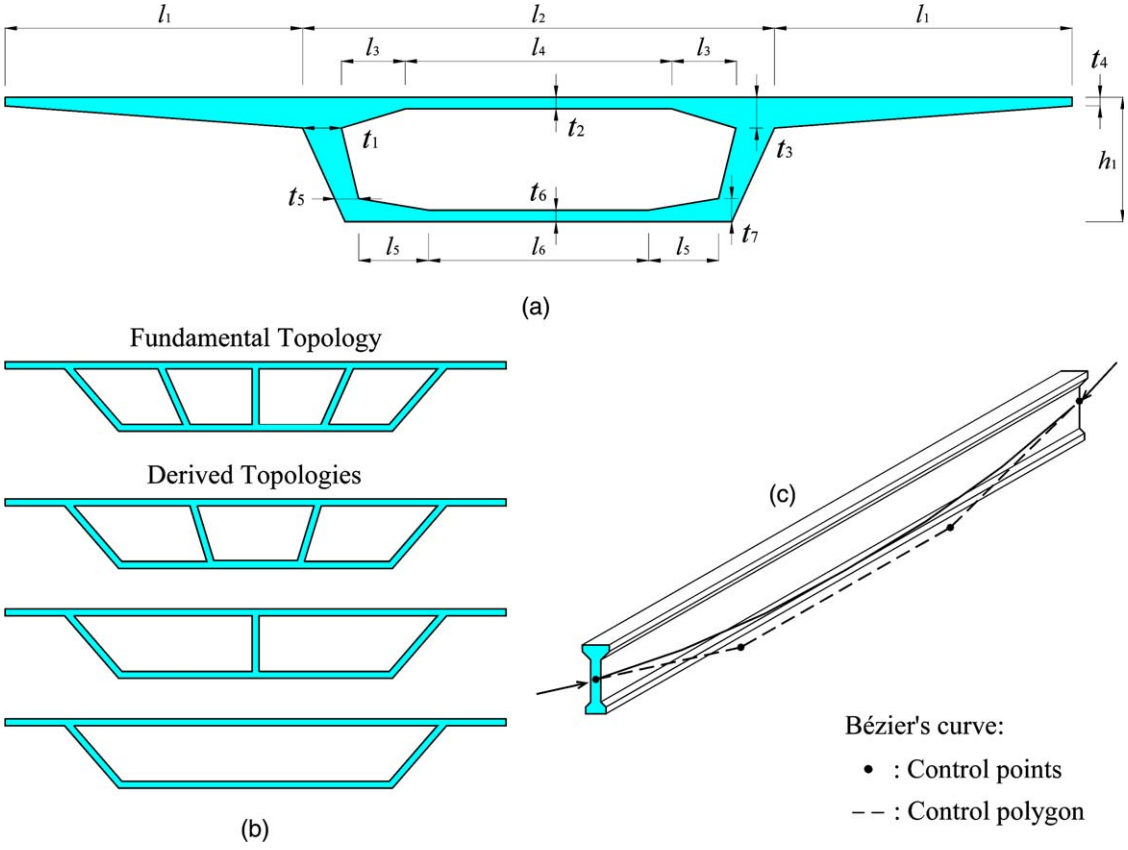

Fig. 3. Choice of the design variables. (a) Geometry: coordinates of the nodal lines and thickness of the finite elements; (b) Topology: structural configuration; (c) Prestressing system: intensity of the prestressing forces and coordinates of the control points of the cables profile.

finite strips. In particular, by assuming the thickness of each plate as linearly varying, the thickness values at the nodal lines completely define the thickness distribution over the whole structure.
- The *structural topology* depends on the mutual arrangement of the strips. In this sense, several alternative structural topologies, for example, identified through an integer variable, need to be considered during the design process. This can be done by building a family of derived topologies by the elimination of one or more folded plates from a given basic topology.
- The *prestressing system* is represented by a set of post-tensioned cables at one or both of their ends and it is fully defined by the intensity of the prestressing forces and by the longitudinal profile of the cables. In this study, the curvilinear profile of the cables is described by means of Bézier's curves [10], which are polynomial curves of degree $n \geq 2$ defined by the position of $n+1$ control points.

Based on the above mentioned criteria, in the proposed formulation, the components of the design vector $\mathbf{x}$ can be identified as quantities belonging to one of the following classes:

(a) Geometry: coordinates of the nodal lines and thickness of the finite elements;
(b) Topology: integer value which identifies the structural configuration;
(c) Prestressing system: intensity of the prestressing forces and coordinates of the control points which define the cables profile.

2.2. Definition of the behavioral design constraints

The dimensions and the components of the vectors $\boldsymbol{g}(\boldsymbol{x})$ and $\boldsymbol{h}(\boldsymbol{x})$ are clearly depending on the particular design problem which has to be solved. They represent some restrictions on the system behavior or performance, expressed as a function of the design variables both in explicit and implicit way. In particular, the structural performance at the serviceability stage usually drives the design process for the class of structures considered here. Therefore, since the structural response under the serviceability loads can be effectively modeled in the linear elastic range, the behavioral design constraints $\boldsymbol{g}(\boldsymbol{x}) \leq \mathbf{0}$ and $\boldsymbol{h}(\boldsymbol{x}) = \mathbf{0}$ assumed in the proposed formulation deal with both the static and kinematic fields evaluated by means of a linear elastic analysis.

With respect to the static field, the stress state $\boldsymbol{s} = \boldsymbol{s}(\boldsymbol{x})$ must not lead to mechanical crisis related for example to the local rupture of the materials. For the special class of structures investigated here, the total stress field is generally given by the superposition of a transversal behavior, mainly regulated by the bending stresses at the local level, and of a longitudinal behavior, mainly regulated by the membrane stress field at the global level. For this reason, the failure conditions on both the membrane $\boldsymbol{s}_a = \boldsymbol{s}_a(\boldsymbol{x}) = [n_x \quad n_y \quad n_{xy}]^{\mathrm{T}}$ and bending $\boldsymbol{s}_b = \boldsymbol{s}_b(\boldsymbol{x}) = [m_x \quad m_y \quad m_{xy}]^{\mathrm{T}}$ stress fields, referred to the directions of orthotropy for non-isotropic structures, are assumed to be independent between them and defined by the following design constraints:

$$\boldsymbol{g}(\boldsymbol{x}) = \begin{bmatrix} \boldsymbol{g}_a(\boldsymbol{x}) \\ \boldsymbol{g}_b(\boldsymbol{x}) \end{bmatrix} = \left[\begin{array}{c} -n_x^- - n_x \\ n_x - n_x^+ \\ -n_y^- - n_y \\ n_y - n_y^+ \\ n_{xy}^2 - (n_x^+ - n_x)(n_y^+ - n_y) \\ n_{xy}^2 - (n_x^- + n_x)(n_y^- + n_y) \\ \hline -m_x^- - m_x \\ m_x - m_x^+ \\ -m_y^- - m_y \\ m_y - m_y^+ \\ m_{xy}^2 - (m_x^+ - m_x)(m_y^+ - m_y) \\ m_{xy}^2 - (m_x^- + m_x)(m_y^- + m_y) \end{array}\right] \leq \mathbf{0} \quad (2)$$

where the non-negative quantities n_x^-, n_x^+, n_y^-, n_y^+ and m_x^-, m_x^+, m_y^-, m_y^+ represent the limit values for the elementary stress states of mono-axial tension/compression and simple shear for the membrane and the bending stress fields respectively. In particular, the constraints $\boldsymbol{g}_a(\boldsymbol{x}) \leq \mathbf{0}$ and $\boldsymbol{g}_b(\boldsymbol{x}) \leq \mathbf{0}$ are described in the stress space, by two limit surfaces, $\mathfrak{I}(\boldsymbol{s}_a) = 0$ and $\mathfrak{I}(\boldsymbol{s}_b) = 0$ for the membrane and bending stress field, respectively, each of them defined by a couple of cones as shown in Fig. 4 [11]. When the hypothesis of independent failure conditions cannot be assumed, a limit surface $\mathfrak{I}(\mathbf{s}) = 0$ taking into account the interaction of the membrane and bending stress fields can also be effectively derived from a linear interpolation of the limit surfaces $\mathfrak{I}(\boldsymbol{s}_a) = 0$ and $\mathfrak{I}(\boldsymbol{s}_b) = 0$. Clearly, the constraints $\boldsymbol{g}(\boldsymbol{x}, r, y) \leq \mathbf{0}$ must be verified for each loading condition r and in each point of the structures, or along the longitudinal coordinate y of each finite strip. In order to reduce the problem to algebraic form, the constraints are verified only in a finite number of transversal cross-sections.

From the kinematic point of view, the displacement field $\boldsymbol{d} = \boldsymbol{d}(\boldsymbol{x})$ should not lead to loss of form. For this purpose, it is introduced a suitable measure of deformation represented by a local *deformability index* $\delta = \delta(\boldsymbol{x},r,y)$ of the cross-sections:

$$\delta(\boldsymbol{x},r,y) = \min_{-\pi \leq \alpha \leq \pi} \frac{\|\boldsymbol{d}(\boldsymbol{x},r,y) - \boldsymbol{d}_0(\boldsymbol{x},r,y,\alpha)\|}{\|\boldsymbol{d}(\boldsymbol{x},r,y)\|} \quad (3)$$

and by a global *deformability index* $\delta = \delta(\boldsymbol{x},r)$ of the

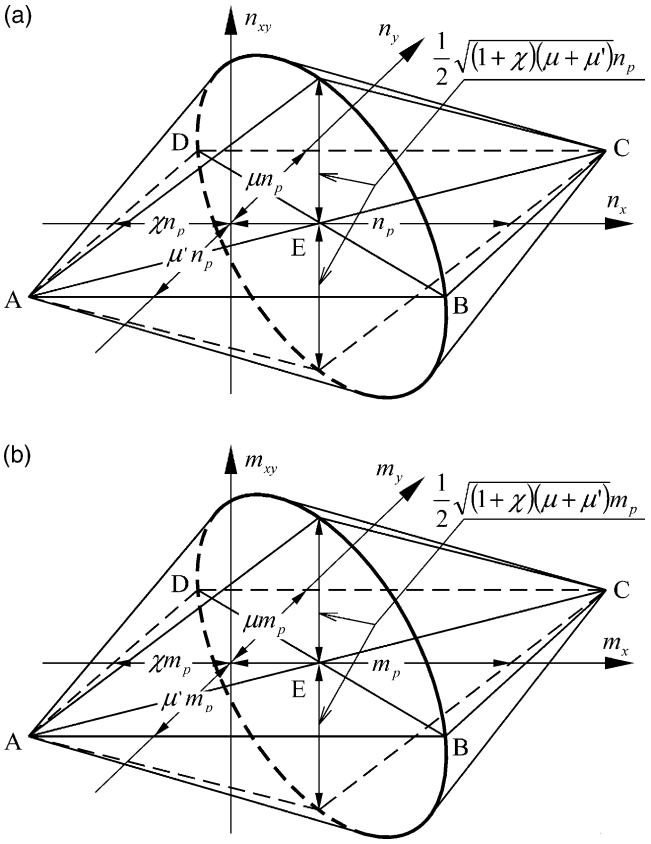

Fig. 4. Limit surfaces (a) $\Im(\boldsymbol{s}_a) = 0$ and (b) $\Im(\boldsymbol{s}_b) = 0$, associated to the limit states on the membrane and bending stress field, respectively ($n_x^+ = n_p$, $n_x^- = \chi n_p$, $n_y^+ = \mu n_p$, $n_y^- = \mu' n_p$; $m_x^+ = m_p$, $m_x^- = \chi m_p$, $m_y^+ = \mu m_p$, $m_y^- = \mu' m_p$).

structure:

$$\delta(\boldsymbol{x},r) = \frac{1}{L}\int_0^L \delta(\boldsymbol{x},r,y)\mathrm{d}y \tag{4}$$

where $\boldsymbol{d} = \boldsymbol{d}(\boldsymbol{x},r,y)$ is the nodal displacement vector of the cross-section at the longitudinal location y for the loading condition r, $\boldsymbol{d}_0 = \boldsymbol{d}_0(\boldsymbol{x},r,y,\alpha)$ is the same vector associated to a rigid rotation α of the undeformed cross-section around its center of gravity in the deformed configuration, the operator $||\cdot||$ denotes the Euclidean vector norm, and L is the longitudinal length of the structure. In particular, the deformability indices δ give a measure of the deformability of both the cross-sections and the structure, respectively. Their values may vary between 0 and 1, which represent the limiting situations of rigid and infinitely deformable structural configuration, respectively. Based on these indices, the structure is enforced to maintain a sufficient rigidity by introducing an indirect constraint on the maximum value of the global *deformability index* $\delta = \delta(\boldsymbol{x})$:

$$\delta(\boldsymbol{x}) = \max_r \delta(\boldsymbol{x},r) \le \delta_{\max} \tag{5}$$

where $\delta_{\max}$ is a suitable upper bound of the index $\delta(\boldsymbol{x})$. The corresponding behavior design constraint is then formulated as follows:

$$g_c(\boldsymbol{x}) = \delta(\boldsymbol{x}) - \delta_{\max} \le 0 \tag{6}$$

2.3. Choice of the objective function

Several quantities able to represent the structural performance may be chosen as target requirements for optimal design. A proper choice of the objective function depends on the nature of the problem and represents a strategic phase of the optimization process. In this paper, attention is focussed on both the material volume and the prestressing force, considered to be the main aspects which contribute to define the total cost of the structure. The objective function is then chosen as a linear combination of the total volume $V(\boldsymbol{x})$ of the structure and the weighted prestressing force $P(\boldsymbol{x}) = \sum_i \beta_i P_i(\boldsymbol{x})$ as follows:

$$\begin{aligned} f(\boldsymbol{x}) &= w_V f_V(\boldsymbol{x}) + w_P f_P(\boldsymbol{x}) \\ &= w_V \frac{V(\boldsymbol{x})}{V(\boldsymbol{x}_0)} + w_P \frac{P(\boldsymbol{x})}{P(\boldsymbol{x}_0)} \end{aligned} \tag{7}$$

where β_i is the weight associated to the prestressing force of the cable i ($\sum_i \beta_i = 1.0$), w_V and w_P are weights which express the relative importance of the dimensionless objective functions $f_V(\boldsymbol{x})$ and $f_P(\boldsymbol{x})$, respectively, and $\boldsymbol{x}_0$ is a reference vector of initial design.

3. Numerical solution of the optimization problem

The optimization problem previously formulated is solved by using a numerical technique derived by the so-called complex method [2,12] which is, as known, a deterministic non-linear mathematical programming procedure. The complex algorithm falls in the class of direct or zero-order methods, since it does not require derivatives but only the evaluation of the involved functions. Such characteristic makes the search process very effective for the solution of the problems investigated in the present study, where the relationship between the objective function and the design variables is generally only available in an implicit form. In the following, some details about the numerical algorithm and the related solution process are given.

3.1. The complex method

The complex method is based on the generation of a sequence of *complexes*. A complex is a geometrical figure consisting of $k \ge n+1$ vertices, of the segments interconnecting them and of the related polygonal areas that enclose a region of the n-dimensional design space. Clearly, only the non-degenerate complexes, i.e. those which enclose a non-zero volume, are feasible for the development of the numerical procedure.

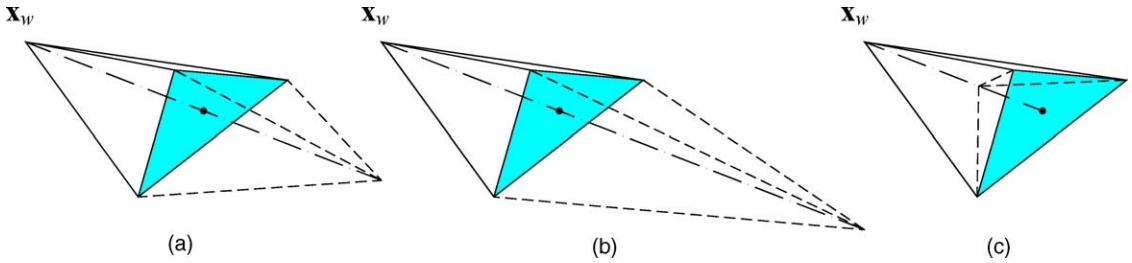

Fig. 5. Basic steps of the complex method: (a) reflection; (b) expansion, and (c) contraction.

The basic idea of the method consists in comparing the values assumed by the objective function in correspondence of the $k \geq n+1$ vertices of the complex and, in a second time, in moving the worst vertex $\boldsymbol{x}_w$ in such a way that some improvement is achieved (Fig. 5). In particular, after an initial complex is heuristically defined, the method moves towards an optimal solution through several basic steps which start with the reflection of the worst vertex $\boldsymbol{x}_w$, or the vertex associated to the largest value of the objective function, through the opposite face of the complex (Fig. 5(a)). If the new vertex is again the worst, an improvement is obtained through an expansion (Fig. 5(b)) or a contraction (Fig. 5(c)). On the contrary, a new vertex is selected and the procedure is repeated until an optimal solution is found. In this way, instead of improving the best result, the search strategy works by eliminating the worst one. Clearly, at each iteration, the basic steps need to be properly modified in order to enforce the path of the search process into the feasible region of the design space. As a concluding remark, it is outlined that a proper selection of the number of vertices usually requires $k \cong 2n$. Moreover, the center of gravity of the initial complex can be assumed as a good choice for the reference vector of initial design $\boldsymbol{x}_0$.

3.2. Convergence criteria

The capability of the complex method in exploring a wide region of the design space—eventually emphasized by using several restarts of the solution process with different initial complexes—usually leads to avoid points of local minimum. The optimal solution for each restart is considered to be reached when some convergence criteria are satisfied. In particular, two conditions must be contemporarily verified:

(1) The dimensionless ratio ε_1 between the maximum value of the distance of each vertex of the complex $\boldsymbol{x}_i$ from its center of gravity x_0 and the effective dimensions of the admissible region is lower than a specified tolerance $\varepsilon_{1,\max}$, or:

$$\varepsilon_1 = \max_{i=1,\ldots,k} \left\| \Delta \boldsymbol{x}^{-1} (\boldsymbol{x}_i - \boldsymbol{x}_0) \right\| \leq \varepsilon_{1,\max} \tag{8}$$

where

$$\Delta \boldsymbol{x} = \begin{bmatrix} \Delta x_1 & 0 & \cdots & 0 \\ 0 & \Delta x_2 & \cdots & 0 \\ \cdots & \cdots & \cdots & \cdots \\ 0 & 0 & \cdots & \Delta x_n \end{bmatrix}, \quad \text{with}$$

$$\Delta x_j = x_j^+ - x_j^-, \quad j = 1,2,\ldots,n \tag{9}$$

(2) The dimensionless standard deviation ε_2 of the values of the objective function $f(\boldsymbol{x}_i)$, computed at the vertices of the complex $i = 1,2,\ldots,k$, with respect to the reference value $f(\boldsymbol{x}_0)$ is lower than a specified tolerance $\varepsilon_{2,\max}$, or:

$$\varepsilon_2 = \sqrt{\frac{1}{k}\sum_{i=1}^{k}\left[\frac{f(\boldsymbol{x}_i) - f(\boldsymbol{x}_0)}{f(\boldsymbol{x}_0)}\right]^2} = \sqrt{\frac{1}{k}\sum_{i=1}^{k}\left[\frac{f(\boldsymbol{x}_i)}{f(\boldsymbol{x}_0)} - 1\right]^2} \leq \varepsilon_{2,\max} \tag{10}$$

3.3. Scaling of the design variables

The complex method has been proven to be very effective in structural optimization. However, especially due to the different nature of the involved quantities, a proper scaling of the design variables should be adopted in order to avoid numerical problems of ill-conditioning. To this aim, the design vector $\boldsymbol{x}$ is expressed as a function of its physical limits $\boldsymbol{x}^-$ and $\boldsymbol{x}^+$ as follows:

$$\boldsymbol{x} = \boldsymbol{x}^- + \boldsymbol{Y}(\boldsymbol{x}^+ - \boldsymbol{x}^-) \tag{11}$$

and the non-zero dimensionless components of the diagonal matrix $\boldsymbol{Y}$ which vary in the range [0;1], are assumed as new scaled design variables.

4. Applications

As already mentioned, in the optimal design of thin-walled folded plates structures for which both the geometry and material properties are constant along a coordinate direction, straight or curved, the choice of the structural morphology consists in defining both the geometry and topology of the cross-section perpendicular to such direction. In addition, the layout of the prestressing system, when it is present, must be also defined. Considering such a context, some design

applications are now presented and briefly described in order to highlight the effectiveness of the proposed design methodology. Such applications are all developed with reference to the following assumption:

- The behavior of the material, assumed to be isotropic and linear elastic, is defined by the Young modulus $E = 30.0$ GPa and the Poisson coefficient $v = 0.15$. The self-weight of the structure is defined by a weight density $\gamma = 25.0$ kN/m^3. For the prestressing system, the instantaneous losses are evaluated by assuming a friction coefficient between cables and ducts $\mu = 0.2$ and a non-intentional curvature of the cables $K' = 0.005$ rad/m.
- The behavioral design constraints on the stress field are defined by the limit values $n_x^+ = -n_x^- = n_y^+ = -n_y^- = 12.0 \cdot t$ MN/m for the membrane forces and $m_x^+ = -m_x^- = m_y^+ = -m_y^- = 1.2 \cdot t^2$ MNm/m for the bending moments, where t (m) denotes the thickness of the corresponding plate. The minimum thickness $t_{\min} = 0.1$ m is assumed at both the ends of each folded plate.
- The convergence of the search process is regulated by the tolerance coefficients $\varepsilon_{1,\max} = \varepsilon_{2,\max} = 0.01$.

4.1. Prestressed beam

The simply supported beam shown in Fig. 6(a), with length $L = 30.0$ m and cross-section having height $H = 3.0$ m and variable width, is considered. Besides its self-weight, the beam is subjected to a uniform load $q = 100.0$ kN/m, applied at the top side of the cross-section, and to the action of a straight prestressing cable located near the bottom side. The beam is modeled by using 20 finite strip elements having the same geometrical dimensions. The thickness distribution along the cross-section which minimizes both the total volume and the intensity of the prestressing force ($w_V = w_P = 1.0$), is searched for. The optimal solution is characterized by the shape of the cross-section shown in Fig. 6(b), with a total volume $V(\boldsymbol{x}_{\text{opt}}) = 1.087$ m^3/m and a prestressing force $P(\boldsymbol{x}_{\text{opt}}) = 5.550$ MN.

4.2. Prestressed roof element

The roof element shown in Fig. 7(a), with length $L = 20.0$ m, width $B = 2.5$ m and height $H = 1.0$ m, is considered. A longitudinal straight cable, prestressed with a force $P = 100.0$ kN, is located within the bottom plate. Besides its self-weight and a uniform line load $Q' = 3.0$ kN/m applied at the end of both the lateral wings, the roof element is subjected to two alternative loading conditions shown in Fig. 7(a) and characterized by the uniform loads $q = 2.0$ kN/m^2 and $v = 1.0$ kN/m^2, respectively. The thickness distribution over the cross-section which minimizes the total volume is searched for. To this purpose, a constant thickness is assumed for each plate, with the exception of the lateral wings, for which two alternative solutions, with and without a terminal bulb, are considered.

The optimal solutions are characterized by the shapes of the cross-section shown in Fig. 7(b), (c). It clearly appears that a higher thickness of the end parts of the wings can lead to a lower thickness of all the other plates (Fig. 7(c)). This latter optimal solution has a total volume $V(\boldsymbol{x}_{\text{opt}}) = 0.538$ m^3/m.

4.3. Barrel vault with edge beams

The barrel vault shown in Fig. 8(a), with length $L = 30.0$ m, width $B = 10.0$ m and constant thickness, is considered. The vault is supported by the two edge beams having a rectangular cross-section with height $h = 1.0$ m. Besides its self-weight, the structure is subjected to two alternative loading conditions shown in Fig. 8(a) and characterized by the uniform loads $q = 3.0$ kN/m^2 and $v = 1.0$ kN/m^2, respectively. The shape of the vault and the thickness of both the vault and the edge beams which minimize the total volume are searched for. To this purpose, the shape of the vault is described by a third degree polynomial curve defined by the symmetrical location of the control points B and C, as shown in Fig. 8(b). The optimal solution, that is characterized by the shape of the vault

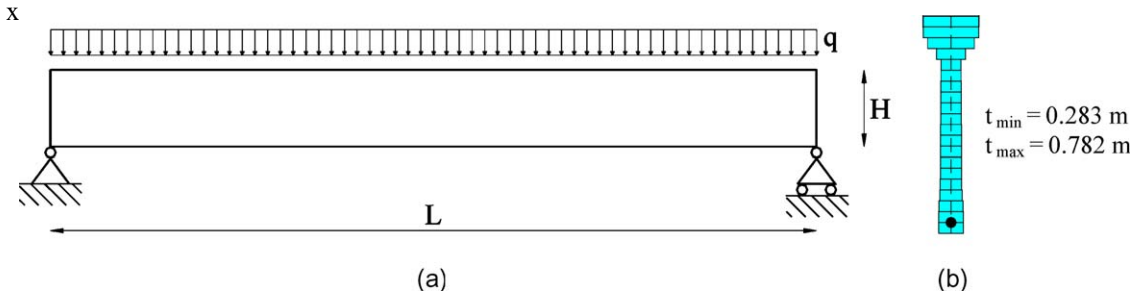

Fig. 6. Prestressed beam. (a) Main dimensions and load. (b) Optimal cross-sectional shape.

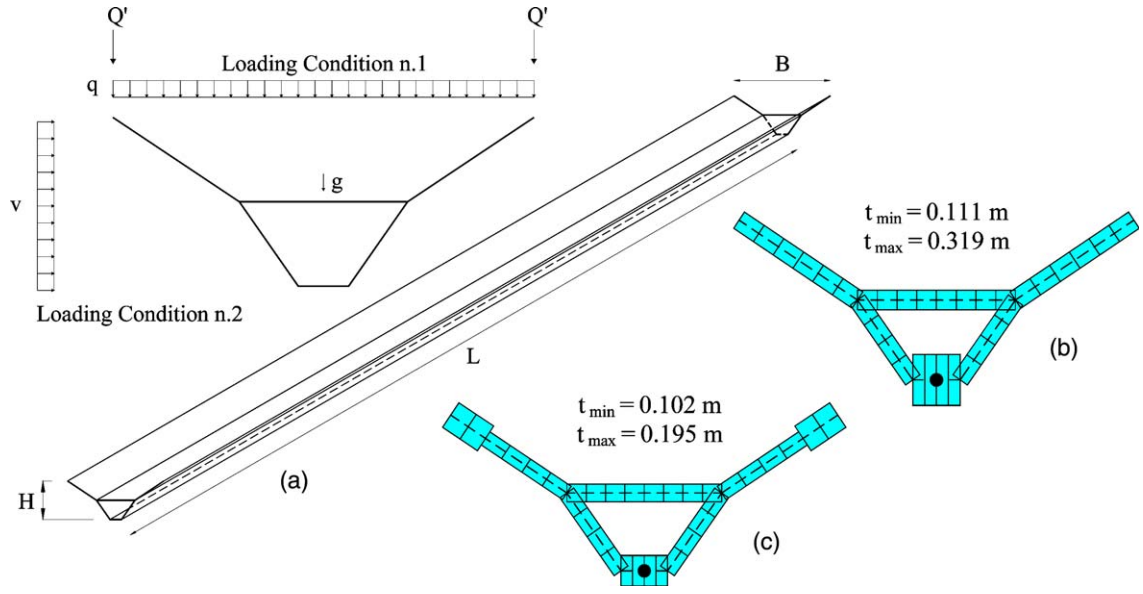

Fig. 7. Roof element. (a) Main dimensions and loads. (b) Optimal thickness distributions, wings with constant thickness and (c) wings with a terminal bulb.

and the thickness distribution shown in Fig. 8(b), has a total volume $V(\boldsymbol{x}_{\text{opt}}) = 0.753\ \text{m}^3/\text{m}$.

4.4. Bridge deck with prestressed girders

The bridge deck shown in Fig. 9(a), with length $L = 40.0$ m, width $B = 12.0$ m and height $H = 3.0$ m, is considered. Besides its self-weight and the weight of the non-structural elements $g_p = 4\ \text{kN/m}^2$, the structure is subjected to the four alternative loading conditions shown in Fig. 9(a), with $q = 8.0\ \text{kN/m}^2$. Both the girders are prestressed with a cable whose profile is described by a third degree polynomial curve. The thickness distribution over the cross-section and the cables profile which minimize both the total volume and the prestressing force ($w_V = w_P = 1.0$), are searched for. To this purpose, the width of the finite strips is assumed to be variable. Moreover, two different constraints for the global deformability index $\delta(\boldsymbol{x})$ are considered, respectively with (1) $\delta_{\max,1} = 0.75$ and (2) $\delta_{\max,2} = 0.50$. The optimal thickness distribution and the cable layout are shown for both cases (1) and (2) in Fig. 9(b) and (c), respectively. The corresponding optimal values of the total volume and of the prestressing force are $V(\boldsymbol{x}_{\text{opt},1}) = 3.783\ \text{m}^3/\text{m}$ and $P(\boldsymbol{x}_{\text{opt},1}) = 7.079$ MN for case (1), $V(\boldsymbol{x}_{\text{opt},2}) = 4.286\ \text{m}^3/\text{m}$ and $P(\boldsymbol{x}_{\text{opt},2}) = 8.482$ MN for case (2). It can be noticed that solution (1), being associated to a less restrictive constraint on the δ-index, leads to lower values of volume and prestressing with respect to solution (2).

In order to better highlight the main aspects of the design process, Figs. 10–14 show the characteristics of the optimal solution (2) and the corresponding evolution of the search procedure. In particular, Fig. 10 shows the distribution along the longitudinal coordinate y of the maximum values attained over all the loading conditions by the components of the behavioral design vectors $\boldsymbol{g}_a(\boldsymbol{x})$ and $\boldsymbol{g}_b(\boldsymbol{x})$, related to the

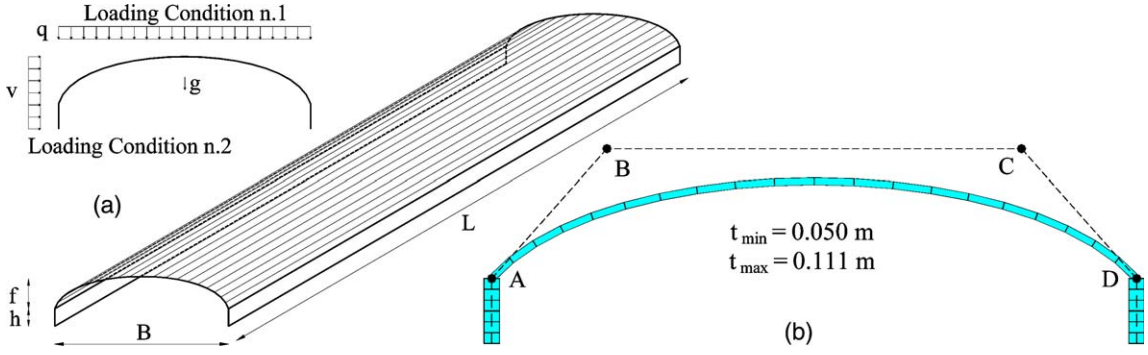

Fig. 8. Barrel vault. (a) Main dimensions and loads; (b) Optimal shape and thickness distribution.

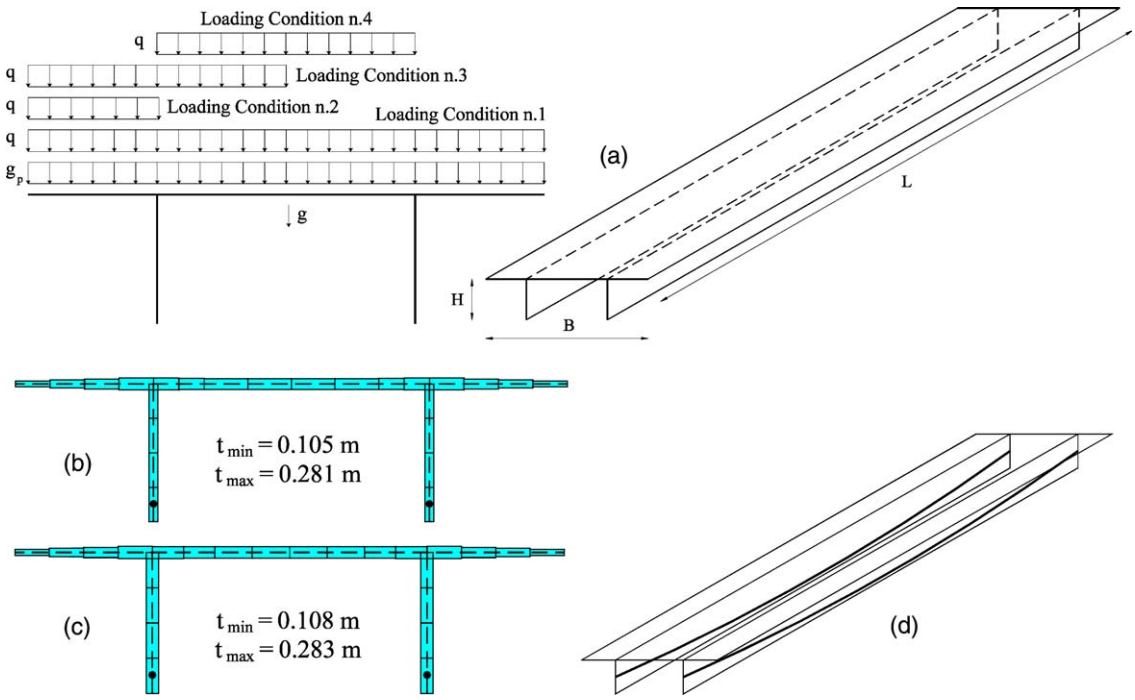

Fig. 9. Bridge deck with girders. (a) Main dimensions and loads. Optimal thickness distribution and cable location at the middle span for (b) $\delta_{max,1} = 0.75$, and (c) $\delta_{max,2} = 0.50$. (d) Optimal cable layout.

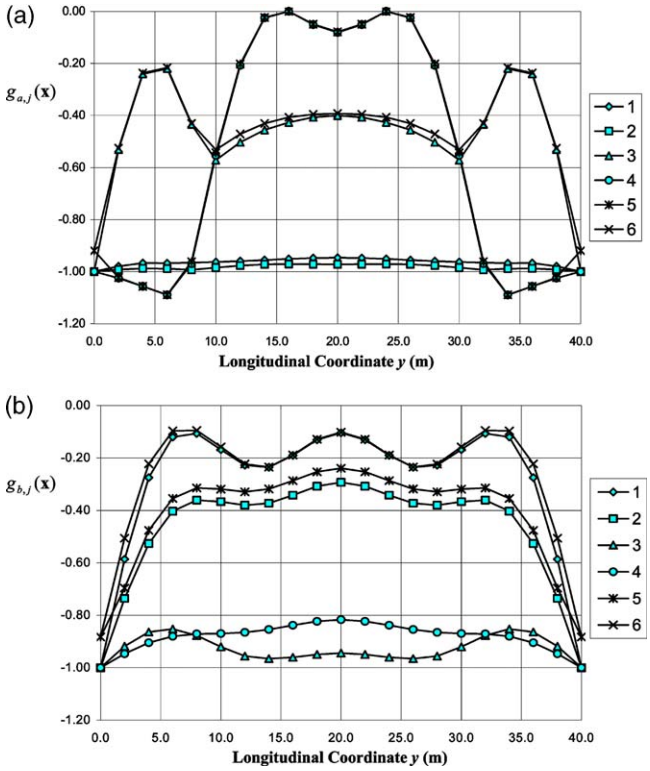

Fig. 10. Bridge deck with girders—case (2). Maximum design constraint values on (a) the membrane static field $g_{a,j}(\boldsymbol{x})$ and (b) the bending static field $g_{b,j}(\boldsymbol{x})$ $(j = 1, \ldots, 6)$.

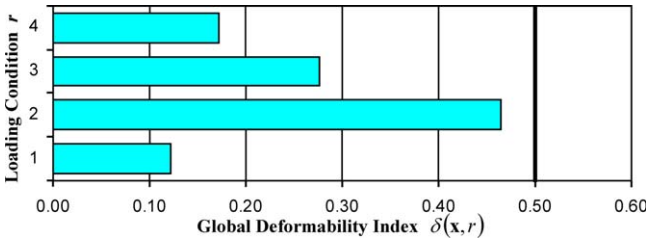

Fig. 11. Bridge deck with girders—case (2). Global deformability index $\delta = \delta(\boldsymbol{x},r)$ of the structure for each loading condition $r = 1, \ldots, 4$.

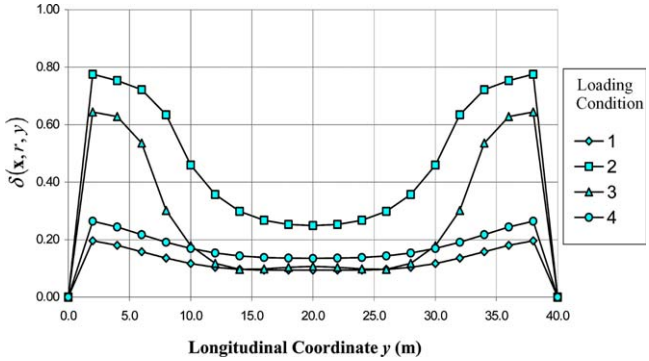

Fig. 12. Bridge deck with girders—case (2). Distribution of the local deformability index of the cross-sections $\delta = \delta(\boldsymbol{x},r,y)$ for each loading condition $r = 1, \ldots, 4$.

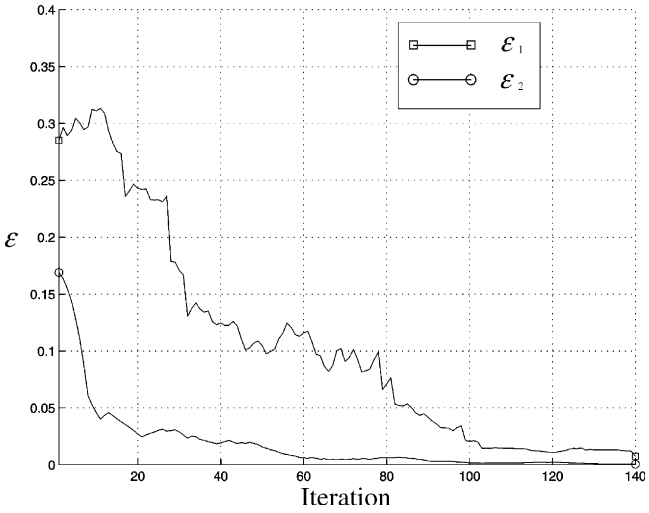

Fig. 13. Bridge deck with girders—case (2). Evolution of the tolerance coefficients ε_1 and ε_2 for convergence criteria.

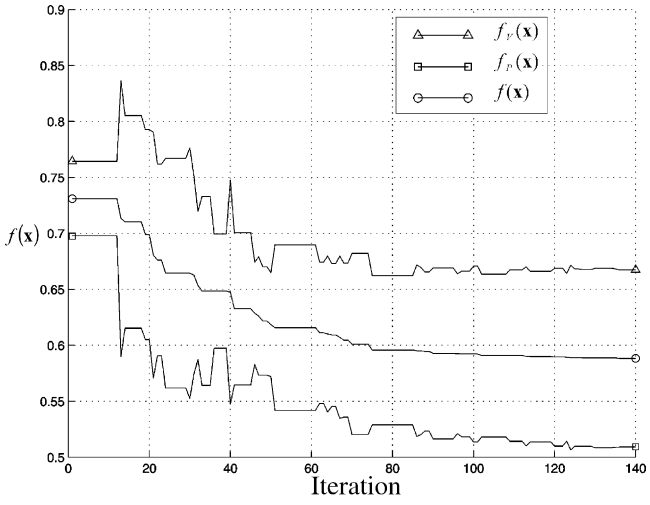

Fig. 14. Bridge deck with girders—case (2). Evolution of the objective function $f(\boldsymbol{x})$ and of its components $f_V(\boldsymbol{x})$ and $f_P(\boldsymbol{x})$ for the current best solution ($w_V = w_P = 1.0$; $V(\boldsymbol{x}_0) = 6.421\ \mathrm{m}^3/\mathrm{m}$, $V(\boldsymbol{x}_{\mathrm{opt}}) = 4.286\ \mathrm{m}^3/\mathrm{m}$; $P(\boldsymbol{x}_0) = 16.654$ kN, $P(\boldsymbol{x}_{\mathrm{opt}}) = 8.482$ kN).

membrane and the bending stress state, respectively. From the inspection of such figures, which highlight the more critical cross-sections with respect to each limit condition, it can be noticed that the design constraints are nowhere violated. Fig. 11 refers instead to the deformability index $\delta(\boldsymbol{x},r)$ which expresses, in an average sense, the kinematic displacement field. Also in this case, it appears that the upper limit $\delta_{\max,2} = 0.50$ is never violated. However, due to the average meaning of the global deformability index, some local violations are expected at the sectional level near the supports for the more demanding loading conditions. This is shown in Fig. 12, which refers to the local deformability index $\delta = \delta(\boldsymbol{x},r,y)$ computed for each cross-section.

With reference to the path of the search process, Fig. 13 shows the evolution of the parameters ε_1 and ε_2

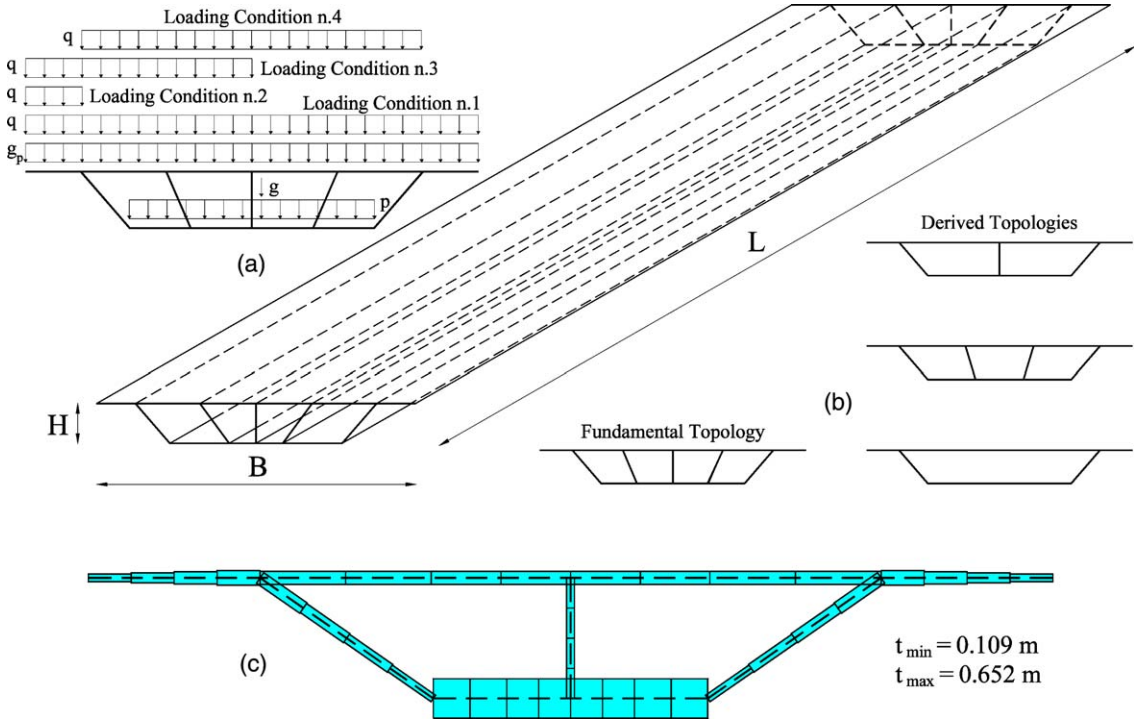

Fig. 15. Box-girder bridge with internal diaphragms. (a) Main dimensions and loads. (b) Cross-sectional topologies. (c) Optimal shape, topology and thickness distribution.

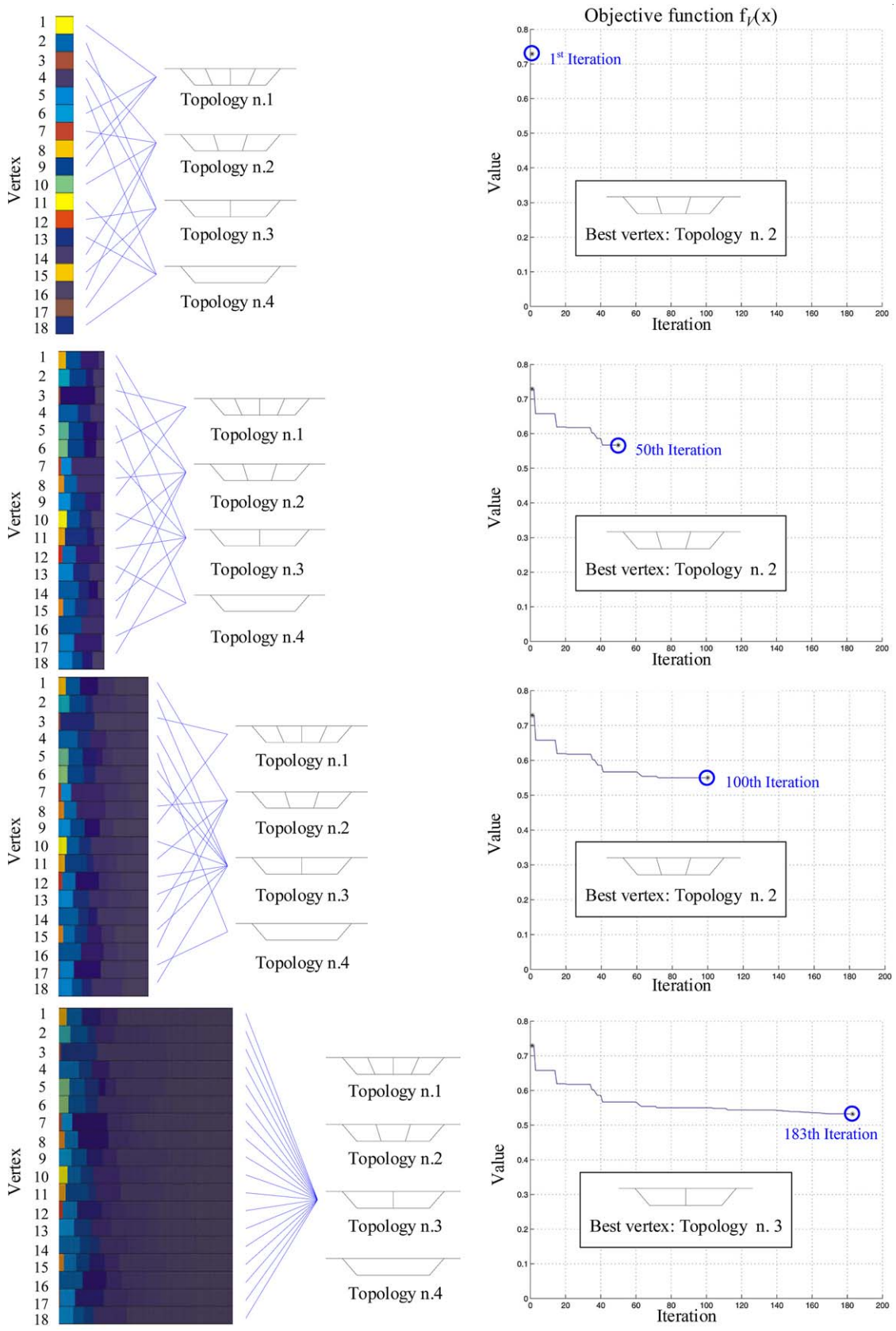

Fig. 16. Box-girder bridge with internal diaphragms. Distribution of the topologies at the vertices of the complex and evolution of the objective function $f(\boldsymbol{x}) \equiv f_V(\boldsymbol{x})$ for the current best solution.

adopted to check the convergence of the iterative procedure. Finally, Fig. 14 shows the corresponding evolution of the objective function $f(\boldsymbol{x})$ and of its components $f_V(\boldsymbol{x})$ and $f_P(\boldsymbol{x})$.

4.5. Box-girder bridge deck with internal diaphragms

The box-girder bridge deck shown in Fig. 15(a), with length $L = 40.0$ m, total width $B = 16.0$ m and height $H = 2.0$ m, is considered. Besides its self-weight, the weight of the non-structural elements $g_p = 4$ kN/m^2 and the service load $p = 2.0$ kN/m^2, the structure is subjected to the four alternative loading conditions shown in Fig. 15(a), with $q = 8$ kN/m^2. The thickness distribution and both the shape and topology of the cross-section which minimize the total volume, are searched for. To this purpose, the topologies associated to the four alternative symmetrical cross-sections shown in Fig. 15(b), each of them derived from the first fundamental one by eliminating or not one or more internal diaphragms, are considered. The search process leads to an optimal solution which corresponds to the two-cellular box girder shown in Fig. 15(c), with a total volume $V(\boldsymbol{x}_{\text{opt}}) = 7.737$ m^3/m. It is worth noting that the high value of thickness of the bottom slab in tension is due to the hypothesis of homogeneous material and elastic behavior. The disposition of proper longitudinal reinforcement, designed with reference to the effective composite and non-linear nature of the material, clearly allows a lower thickness of the concrete slab.

Finally, with reference to the path of the search process, Fig. 16 shows the distribution of the topologies at the vertices of the complex and the evolution of the objective function $f(\boldsymbol{x})$ for the current best solution during the iterative process.

5. Conclusions

The problem of finding the optimal shape, size and topology of prestressed folded plate structures under multiple loading conditions has been investigated. The design problem has been formulated as a mathematical optimization problem, accounting for both static and kinematic constraints, and it has been solved by using a numerical algorithm based on the complex method. The structural analyses needed for the optimization process have been performed by using the finite strip method. A number of applications have shown the effectiveness of the proposed procedure.

In particular, the design tools presented in this paper can usefully be applied at the conceptual design stage, where the designer is usually interested in comparing between them a variety of alternative optimal solutions, derived, for example, by using different design models. These solutions, which the proposed procedure identifies with wide generality, rationality and objectivity, can be then used as a basis for a more detailed design of the reinforcement. Clearly, future developments are expected in order to obtain a better control of the design problem, especially on the definition of the design constraints, which should also account for technological aspects, as well as for aesthetical and additional functional requirements.

References

[1] ASCE. Design of cylindrical concrete shell roofs. Manual of engineering practice. New York (NY): ASCE; 1952, p. 31.
[2] Belegundu AD, Chandrupatla TR. Optimization concepts and applications in engineering. Upper Saddle River (NJ): Prentice-Hall; 1999.
[3] Bergamini A, Biondini F. Optimisation of folded plate structures. Proceedings of the Second International Conference on Advances in Structural Engineering and Mechanics (ASEM02), Seoul, Korea, August 21–23. 2002.
[4] Biondini F, Bontempi F, Malerba PG. Ottimizzazione di forma di strutture a folded-plates. Proceedings of the 13th C.T.E. Conference, Pisa, Italy, November 9–10–11. 2000 [in Italian].
[5] Cheung YK. Finite strip method in structural analysis. Oxford: Pergamon Press; 1976.
[6] Kristek V. Theory of box girder bridges. Prague: John Wiley and Sons; 1979.
[7] Loo YC, Cusens A. The finite strip method in bridge engineering. London: E. & F.N. Spon; 1978.
[8] Malerba PG, Toniolo G. Metodi di discretizzazione dell'analisi strutturale. Milan, Italy: Masson Editore; 1981 [in Italian].
[9] Martinez Y Cabrera F, Menni C. I ponti a cassone monocellulare a profilo deformabile. Technical Report, 33. Istituto di Scienza e Tecnica delle Costruzioni, Politecnico di Milano, Tamburini Editore, Milan, 1974 [in Italian].
[10] Mortenson ME. Mathematics for computer graphics applications. New York (NY): Industrial Press; 1999.
[11] Nielsen MP. Limit analysis and concrete plasticity. Boca Raton (FL): CRC Press; 1999.
[12] Rao SS. Engineering optimization—theory and practice. New York (NY): John Wiley and Sons; 1996.
[13] Schlaich J, Scheef H. Concrete box-girder bridges. Structural engineering documents, 1e. International Association for Bridge and Structural Engineering (IABSE); 1982.